The octagonal type of the quasiperiodic succession algorithm as a recursive formula set which generates the growth of a flawless Ammann-Beenker substitution tiling solely using local information from neighbouring cluster cells

Uli Gaenshirt

Wartburgstraße 2, 90491 Nuremberg, Germany

1. Introduction

In 1973, R. Penrose found a quasiperiodic set of tiles with tenfold rotational symmetry [1].
In 1981, N. G. de Bruijn developed a way to generate quasiperiodicity by projection [2].
One year later, inspired by the work of his teacher de Bruijn, F. P. M. Beenker proposed a tiling of squares and rhombs with octagonal rotational symmetry [3], called the Ammann-Beenker (AB) tiling, due to the equivalent tiling found by Robert Ammann six years before.
In 1984, D. Shechtman et al. described materials inducing diffraction patterns with tenfold rotational symmetry [4] which seemed to be a realization of the above-mentioned works.
In 1987 and 1988, the list of these new materials, now called quasicrystals, was extended by some examples with eightfold rotational symmetry, discovered by Wang, Chen and Kuo.
An alternative way to generate tilings with perfect order is the substitution method [1, 3], which decomposes the tiles into definite arrangements of smaller tiles. But substitution, as well as projection, is a global method and not applicable for modelling quasicrystal growth.
The decagonal covering cluster, proposed by P. Gummelt [5] in 1996, and the octagonal covering cluster (here denoted by Ω), proposed by F. Gähler and S. I. Ben Abraham [6] in 1999, were important innovations in tiling theory. However, the local covering rules of the cluster cells lead inevitably to mismatches as well as the local matching rules of the tiles.
The decagonal quasiperiodic succession algorithm, published in 2007 by U. Gaenshirt & M. Willsch [7], generates a flawless Penrose cartwheel-type tiling [5, 7] although it acts locally.
The octagonal type of succession algorithm which is presented here generates a flawless octagonal AB-substitution tiling resp. a Gähler cluster covering, acting locally just as well.

2. The successive generation of a quasiperiodic 1D-grid Γ^x

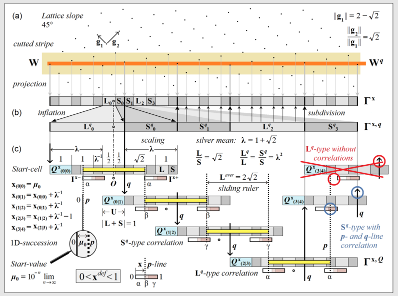

Figure 1. Generation of a 1D-grid Γ^x: (a) cut & project, (b) inflation & subdivision, (c) 1D-succession.

In figure 1 three different methods are adjusted to generate a 1D Ammann bar grid Γ^x.
In the cut & project scheme (figure 1a) the points of a sloped periodic lattice are projected from the inside of a horizontal stripe-shaped window **W** onto a horizontal line.
The substitution method combines inflation & subdivision (figure 1b). The grid intervals **L** and **S** ($\mathbf{L}/\mathbf{S} = \sqrt{2}$) are firstly inflated (enlarged with factor λ^2) to $\mathbf{L}^q$- and $\mathbf{S}^q$-intervals and then subdivided into the sequences **S-L-S-L-S** resp. **S-L-S** (silver mean $\lambda = 1+\sqrt{2}$).
In contrast to the latter global systems, the 1D-succession (figure 2c) acts locally. The cell grid $\Gamma^{x,Q}$ of a cell Q^x writes: U-S-L-S-L-S-(q-line)-S-L-S-L-S, with $\mathbf{U} = [\mathbf{L}+\mathbf{S}]$. The twin-scale $\mathbf{I}^{x\pm}$ consists on two single scales $\mathbf{I}^{x+}$ and $\mathbf{I}^{x-}$. Their value-lines p are joined by a sliding ruler. Its length, $\mathbf{L}^{aver}$, is the average of the q-line grid intervals $\mathbf{L}^q$ and $\mathbf{S}^q$, with respect to the ratio $\sqrt{2}$:1 of their length and 1:$\sqrt{2}$ of their frequency rate in an infinitely expanded grid $\Gamma^{x,q,\infty}$.
The cell grids $\Gamma^{x,Q}$ and the twin-scales $\mathbf{I}^{x\pm}$ allow two kinds of cell correlation with different results for the value x^{succ} of a successor cell relative to the value x^{pred} of a predecessor cell.

$\mathbf{S}^q$-type: $x^{succ} = x^{pred} + \lambda^{-1}$ $\quad$ $\mathbf{L}^q$-type: $x^{succ} = x^{pred} + \lambda^{-1} - 1$ $\quad$ condition: $0 < x^{def} < 1$

The value condition always restricts the two possibilities of cell correlation to a single one.
The created sequence is in accordance to the grid Γ^x generated by the global systems.

3. Construction of the Ammann bar 8-grid Γ and cell grid Γ^Q

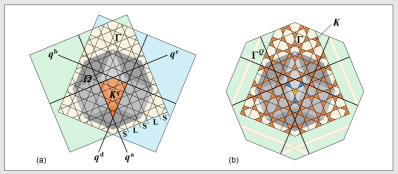

Figure 2. (a) Gähler-octagon Ω with Ammann bar 8-grid Γ and kite K^q. (b) Octagonal cell grid Γ^Q.

The grey marked octagon in the center of figure 2a is a Gähler-octagon Ω [6], a unit cell of the quasiperiodic Ammann-Beenker tiling. The superposed Ammann lines q^a, q^b, q^c, q^d, which enclose the orange kite K^q, have an equivalent relation to the Gähler-octagon Ω.
In accordance to the 1D-cell Q^x (see figure 1c) two bar sequences **S-L-S-L-S** are added on both sides of the Ammann lines q^a, q^b, q^c, q^d and generate the Ammann bar 8-grid Γ.
Figure 2b shows the elementary cell grid Γ^Q of a cluster cell Q. It consists of the grid Γ in the outlines of figure 1a and of the octagon lines. The four lines inside the octagon which occupy alternately positions at the inner resp. outer borders of the white bars are not part of Γ^Q!

4. The seven neighbour transformations h_k of the AB-tiling

Because of $K^q = K \cdot \lambda^2$, and due to the equivalent relations between K^q, Q and Ω, the kites K in figure 2b represent a downscaled substitution-tiling. Each kite K^q is invariably surrounded by three kites. The six neighbour types (figure 3) can be reduced to seven transformations $h_k \in \{h_{\bar{2}}, h_{\bar{3}}, h_{\bar{4}}, h_1, h_2, h_3, h_4\}$, as imaged in figure 4 (the inverses h_k^{-1} are denoted by $h_{\bar{k}}$).
From the scaling in figure 1c results an edge length $a_B = \sqrt{2}$ of the Ammann-Beenker tiles.
The distances between the cell centers can be calculated to: $l = 2\sqrt{2}\cos \pi/8$ and $s = \sqrt{2}$.
With $z \in \mathbb{C}$, $\mathrm{i}^2 = -1$ and $\mathbf{E}^2 \to \mathbf{E}^2$ the transformations h_k can be written as follows:

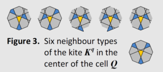

Figure 3. Six neighbour types of the kite K^q in the center of the cell Q

$h_1(z) = z\cdot(-1) + l\cdot(-\mathrm{i})$
$h_2(z) = z\cdot(0{,}5\sqrt{2} - \mathrm{i}\,0{,}5\sqrt{2}) + l\cdot(0{,}5\sqrt{2} + \mathrm{i}\,0{,}5\sqrt{2})$
$h_{\bar{3}}(z) = z\cdot(0{,}5\sqrt{2} + \mathrm{i}\,0{,}5\sqrt{2}) + l\cdot(-\mathrm{i})$
$h_{\bar{2}}(z) = z\cdot(0{,}5\sqrt{2} + \mathrm{i}\,0{,}5\sqrt{2}) + s\cdot(\cos \pi/8 + \mathrm{i}\sin \pi/8)$
$h_3(z) = z\cdot(0{,}5\sqrt{2} - \mathrm{i}\,0{,}5\sqrt{2}) + s\cdot(-\cos \pi/8 + \mathrm{i}\sin \pi/8)$
$h_4(z) = z\cdot(0{,}5\sqrt{2} - \mathrm{i}\,0{,}5\sqrt{2}) + l\cdot(-\mathrm{i})$
$h_{\bar{4}}(z) = z\cdot(0{,}5\sqrt{2} + \mathrm{i}\,0{,}5\sqrt{2}) + l\cdot(-0{,}5\sqrt{2} + \mathrm{i}\,0{,}5\sqrt{2})$

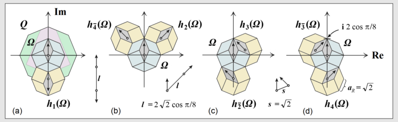

Figure 4. The seven transformations h_k, represented by Ω. (a) h_1, (b) $h_{\bar{4}}$, h_2, (c) h_3, $h_{\bar{2}}$, (d) $h_{\bar{3}}$, h_4.

5. The cluster cell Q and its correlations with a cell $h_2(Q)$

The cell grid Γ^Q is a superposition of four 1D-cell grids $\Gamma^{a,Q}$, $\Gamma^{b,Q}$, $\Gamma^{c,Q}$, $\Gamma^{d,Q}$ which coincide with the arrangement of the Ammann lines q^a, q^b, q^c, q^d in a Gähler-octagon Ω (figure 2a, b).
A fixation of four twin-scales $\mathbf{I}^{a\pm}$, $\mathbf{I}^{b\pm}$, $\mathbf{I}^{c\pm}$, $\mathbf{I}^{d\pm}$ (figure 1c) on the cell grid Γ^Q creates the cluster cell Q (figure 5a) which is consequently a superposition of four 1D-cells Q^a, Q^b, Q^c, Q^d.
Thus the cluster cells Q generate four 1D-grids Γ^a, Γ^b, Γ^c, Γ^d which add up to the grid Γ.
The scale value implications, pictured in the center of figure 5a (formulae at the end of text), are derived from a globally generated grid Γ. They finally enable unambiguous calculations.

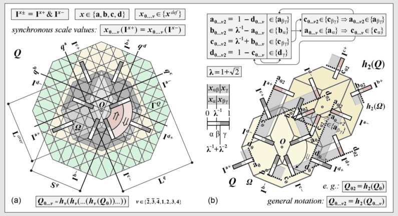

Figure 5. (a) Cluster cell Q with four twin-scales $\mathbf{I}^{x\pm}$. (b) Twin-scale correlation of the cells Q and $h_2(Q)$

For lucidity the correlating twin-scales $\mathbf{I}^{a\pm}$, $\mathbf{I}^{b\pm}$, $\mathbf{I}^{c\pm}$, $\mathbf{I}^{d\pm}$ of Q and $h_2(Q)$ in figure 5b are directly fixed on the equivalent Gähler-octagons Ω and $h_2(\Omega)$. The grey bars, connecting the scales of both cells, represent the scope of the permitted scale values of the transformation h_2.
The dotted p-lines (compare figure 1c) represent the value correlation of Q_0 and $Q_{02} = h_2(Q_0)$.
The four-line table at the top contains the correlation equations of the transformation h_2.
The value restrictions α, β, γ therein are derived from the first two scale value implications:

$\lambda^{-1} < \mathbf{c} \Rightarrow \lambda^{-1} < \mathbf{a}$ $\quad$ $\mathbf{a} < \lambda^{-1} \Rightarrow \mathbf{c} < \lambda^{-1}$ $\quad$ $\lambda^{-1} < \mathbf{b} \Rightarrow \lambda^{-1} < \mathbf{d}$ $\quad$ $\mathbf{d} < \lambda^{-1} \Rightarrow \mathbf{b} < \lambda^{-1}$

6. The octagonal quasiperiodic succession algorithm

The recursive formula set (table 1) consists on one h_ν- and seven h_k-modules. A verified h_k-transformation is named h_ν. A cell with a verified path from the start-cell Q_0 is termed $Q_{0\ldots\nu}$.
The four values $x_{0\ldots\nu}$ in the h_ν-module, with $x \in \{\mathbf{a}, \mathbf{b}, \mathbf{c}, \mathbf{d}\}$, are the values $x^{pred}_{0\ldots\nu k}$ of a verified predecessor cell. The numbers k of $x^{pred}_{0\ldots\nu k}$ are renamed to the numbers ν of $x_{0\ldots\nu}$.
The h_k-modules contain four correlation equations each (see derivation for h_2 in figure 5b).
The ternary relations restrict the allowed values x_k^{def} and lead to the following truth values t:

$x_{0\ldots\nu k} \in \{x_k^{def}\} \Rightarrow t(x_{0\ldots\nu k}) = \mathrm{T}$ $\quad$ $x_{0\ldots\nu k} \notin \{x_k^{def}\} \Rightarrow t(x_{0\ldots\nu k}) = \mathrm{F} \Rightarrow t(Q_{0\ldots\nu k}) = \mathrm{F}$ *forbidden*

$t(\mathbf{a}_{0\ldots\nu k}) = \mathrm{T}$, $t(\mathbf{b}_{0\ldots\nu k}) = \mathrm{T}$, $t(\mathbf{c}_{0\ldots\nu k}) = \mathrm{T}$, $t(\mathbf{d}_{0\ldots\nu k}) = \mathrm{T} \Rightarrow t(Q_{0\ldots\nu k}) = \mathrm{T}$ *verified*

Only values of a verified cell may be inserted into the h_ν-module of a successor formula set.
Table 1 shows the formula set with the exemplarily inserted start-values of the start-cell Q_0: $\mathbf{a}_0 = \mathbf{b}_0 = \mathbf{c}_0 = \mathbf{d}_0 = \mu_0 = 10^{-n}$, $\lim n \to \infty$ (The infinitesimal start-values prohibit ambiguity).
The neighbour cells of the start cell Q_0 are calculated to $Q_{0\bar{4}}$, Q_{01} and Q_{02}, in accordance to the substitution structure (Compare the three blue kites K in the center part of figure 2b).

Table 1. The h_ν-module and the seven h_k-modules with the inserted values μ_0 of the start-cell Q_0.

h_ν	$Q_{0\ldots\nu}$ =	Q_0 (start-cell)	verified predecessor cell	⇐ $t(Q_{0\ldots\nu})$ =	T	⇐
	$\mathbf{a}_{0\ldots\nu}$ =	μ_0	verified predecessor value	$t(\mathbf{a}_{0\ldots\nu})$ =	T	↑
	$\mathbf{b}_{0\ldots\nu}$ =	μ_0	verified predecessor value	$t(\mathbf{b}_{0\ldots\nu})$ =	T	↑
	$\mathbf{c}_{0\ldots\nu}$ =	μ_0	verified predecessor value	$t(\mathbf{c}_{0\ldots\nu})$ =	T	↑
	$\mathbf{d}_{0\ldots\nu}$ =	μ_0	verified predecessor value	$t(\mathbf{d}_{0\ldots\nu})$ =	T	↑

h_k — the values of the h_ν-module have to be inserted into the h_k-modules

$h_{\bar{2}}$	$Q_{0\ldots\nu\bar{2}}$ =	$Q_{0\bar{2}}$	forbidden successor cell	⇐ $t(Q_{0\ldots\nu\bar{2}})$ =	F	⇐
	$\mathbf{a}_{0\ldots\nu\bar{2}} = \lambda^{-1} - \mathbf{b}_{0\ldots\nu}$ =	$\lambda^{-1} - \mu_0$	$0 < \mathbf{a}_{\bar{2}}^{def} < \lambda^{-1}$	⇒ $t(\mathbf{a}_{0\ldots\nu\bar{2}})$ =	T	↑
	$\mathbf{b}_{0\ldots\nu\bar{2}} = -\lambda^{-1} + \mathbf{c}_{0\ldots\nu}$ =	$-\lambda^{-1} + \mu_0$	$0 < \mathbf{b}_{\bar{2}}^{def} < \lambda^{-1}$	⇒ $t(\mathbf{b}_{0\ldots\nu\bar{2}})$ =	F	↑
	$\mathbf{c}_{0\ldots\nu\bar{2}} = 1 - \mathbf{d}_{0\ldots\nu}$ =	$1 - \mu_0$	$0 < \mathbf{c}_{\bar{2}}^{def} < \lambda^{-1}$	⇒ $t(\mathbf{c}_{0\ldots\nu\bar{2}})$ =	F	↑
	$\mathbf{d}_{0\ldots\nu\bar{2}} = 1 - \mathbf{a}_{0\ldots\nu}$ =	$1 - \mu_0$	$0 < \mathbf{d}_{\bar{2}}^{def} < \lambda^{-1}+\lambda^{-2}$	⇒ $t(\mathbf{d}_{0\ldots\nu\bar{2}})$ =	F	↑
$h_{\bar{3}}$	$Q_{0\ldots\nu\bar{3}}$ =	$Q_{0\bar{3}}$	forbidden successor cell	⇐ $t(Q_{0\ldots\nu\bar{3}})$ =	F	⇐
	$\mathbf{a}_{0\ldots\nu\bar{3}} = \sqrt{2} - \mathbf{d}_{0\ldots\nu}$ =	$\sqrt{2} - \mu_0$	$\lambda^{-1} < \mathbf{a}_{\bar{3}}^{def} < 1$	⇒ $t(\mathbf{a}_{0\ldots\nu\bar{3}})$ =	F	↑
	$\mathbf{b}_{0\ldots\nu\bar{3}} = 1 - \mathbf{a}_{0\ldots\nu}$ =	$1 - \mu_0$	$0 < \mathbf{b}_{\bar{3}}^{def} < 2\lambda^{-1}$	⇒ $t(\mathbf{b}_{0\ldots\nu\bar{3}})$ =	F	↑
	$\mathbf{c}_{0\ldots\nu\bar{3}} = \mathbf{b}_{0\ldots\nu}$ =	μ_0	$0 < \mathbf{c}_{\bar{3}}^{def} < 2\lambda^{-1}$	⇒ $t(\mathbf{c}_{0\ldots\nu\bar{3}})$ =	T	↑
	$\mathbf{d}_{0\ldots\nu\bar{3}} = 1 - \mathbf{c}_{0\ldots\nu}$ =	$1 - \mu_0$	$\lambda^{-2} < \mathbf{d}_{\bar{3}}^{def} < 1$	⇒ $t(\mathbf{d}_{0\ldots\nu\bar{3}})$ =	T	↑
$h_{\bar{4}}$	$Q_{0\ldots\nu\bar{4}}$ =	$Q_{0\bar{4}}$	verified successor cell	⇐ $t(Q_{0\ldots\nu\bar{4}})$ =	T	⇐
	$\mathbf{a}_{0\ldots\nu\bar{4}} = 1 - \mathbf{b}_{0\ldots\nu}$ =	$1 - \mu_0$	$\lambda^{-1}+\lambda^{-2} < \mathbf{a}_{\bar{4}}^{def} < 1$	⇒ $t(\mathbf{a}_{0\ldots\nu\bar{4}})$ =	T	↑
	$\mathbf{b}_{0\ldots\nu\bar{4}} = \lambda^{-1} + \mathbf{c}_{0\ldots\nu}$ =	$\lambda^{-1} + \mu_0$	$\lambda^{-1} < \mathbf{b}_{\bar{4}}^{def} < 2\lambda^{-1}$	⇒ $t(\mathbf{b}_{0\ldots\nu\bar{4}})$ =	T	↑
	$\mathbf{c}_{0\ldots\nu\bar{4}} = \lambda^{-1} - \mathbf{d}_{0\ldots\nu}$ =	$\lambda^{-1} - \mu_0$	$0 < \mathbf{c}_{\bar{4}}^{def} < \lambda^{-1}$	⇒ $t(\mathbf{c}_{0\ldots\nu\bar{4}})$ =	T	↑
	$\mathbf{d}_{0\ldots\nu\bar{4}} = 1 - \mathbf{a}_{0\ldots\nu}$ =	$1 - \mu_0$	$\lambda^{-1} < \mathbf{d}_{\bar{4}}^{def} < 1$	⇒ $t(\mathbf{d}_{0\ldots\nu\bar{4}})$ =	T	↑
h_1	$Q_{0\ldots\nu1}$ =	Q_{01}	verified successor cell	⇐ $t(Q_{0\ldots\nu1})$ =	T	⇐
	$\mathbf{a}_{0\ldots\nu1} = 1 - \mathbf{a}_{0\ldots\nu}$ =	$1 - \mu_0$	$0 < \mathbf{a}_1^{def} < 1$	⇒ $t(\mathbf{a}_{0\ldots\nu1})$ =	T	↑
	$\mathbf{b}_{0\ldots\nu1} = \lambda^{-1} - \mathbf{b}_{0\ldots\nu}$ =	$\lambda^{-1} - \mu_0$	$0 < \mathbf{b}_1^{def} < \lambda^{-1}$	⇒ $t(\mathbf{b}_{0\ldots\nu1})$ =	T	↑
	$\mathbf{c}_{0\ldots\nu1} = \lambda^{-1} - \mathbf{c}_{0\ldots\nu}$ =	$\lambda^{-1} - \mu_0$	$0 < \mathbf{c}_1^{def} < \lambda^{-1}$	⇒ $t(\mathbf{c}_{0\ldots\nu1})$ =	T	↑
	$\mathbf{d}_{0\ldots\nu1} = 1 - \mathbf{d}_{0\ldots\nu}$ =	$1 - \mu_0$	$0 < \mathbf{d}_1^{def} < 1$	⇒ $t(\mathbf{d}_{0\ldots\nu1})$ =	T	↑
h_2	$Q_{0\ldots\nu2}$ =	Q_{02}	verified successor cell	⇐ $t(Q_{0\ldots\nu2})$ =	T	⇐
	$\mathbf{a}_{0\ldots\nu2} = 1 - \mathbf{d}_{0\ldots\nu}$ =	$1 - \mu_0$	$\lambda^{-1} < \mathbf{a}_2^{def} < 1$	⇒ $t(\mathbf{a}_{0\ldots\nu2})$ =	T	↑
	$\mathbf{b}_{0\ldots\nu2} = \lambda^{-1} - \mathbf{a}_{0\ldots\nu}$ =	$\lambda^{-1} - \mu_0$	$0 < \mathbf{b}_2^{def} < \lambda^{-1}$	⇒ $t(\mathbf{b}_{0\ldots\nu2})$ =	T	↑
	$\mathbf{c}_{0\ldots\nu2} = \lambda^{-1} + \mathbf{b}_{0\ldots\nu}$ =	$\lambda^{-1} + \mu_0$	$\lambda^{-1} < \mathbf{c}_2^{def} < 2\lambda^{-1}$	⇒ $t(\mathbf{c}_{0\ldots\nu2})$ =	T	↑
	$\mathbf{d}_{0\ldots\nu2} = 1 - \mathbf{c}_{0\ldots\nu}$ =	$1 - \mu_0$	$\lambda^{-1}+\lambda^{-2} < \mathbf{d}_2^{def} < 1$	⇒ $t(\mathbf{d}_{0\ldots\nu2})$ =	T	↑
h_3	$Q_{0\ldots\nu3}$ =	Q_{03}	forbidden successor cell	⇐ $t(Q_{0\ldots\nu3})$ =	F	⇐
	$\mathbf{a}_{0\ldots\nu3} = 1 - \mathbf{b}_{0\ldots\nu}$ =	$1 - \mu_0$	$\lambda^{-2} < \mathbf{a}_3^{def} < 1$	⇒ $t(\mathbf{a}_{0\ldots\nu3})$ =	T	↑
	$\mathbf{b}_{0\ldots\nu3} = \mathbf{c}_{0\ldots\nu}$ =	μ_0	$0 < \mathbf{b}_3^{def} < 2\lambda^{-1}$	⇒ $t(\mathbf{b}_{0\ldots\nu3})$ =	T	↑
	$\mathbf{c}_{0\ldots\nu3} = 1 - \mathbf{d}_{0\ldots\nu}$ =	$1 - \mu_0$	$0 < \mathbf{c}_3^{def} < 2\lambda^{-1}$	⇒ $t(\mathbf{c}_{0\ldots\nu3})$ =	F	↑
	$\mathbf{d}_{0\ldots\nu3} = \sqrt{2} - \mathbf{a}_{0\ldots\nu}$ =	$\sqrt{2} - \mu_0$	$\lambda^{-1} < \mathbf{d}_3^{def} < 1$	⇒ $t(\mathbf{d}_{0\ldots\nu3})$ =	F	↑
h_4	$Q_{0\ldots\nu4}$ =	Q_{04}	forbidden successor cell	⇐ $t(Q_{0\ldots\nu4})$ =	F	⇐
	$\mathbf{a}_{0\ldots\nu4} = 1 - \mathbf{d}_{0\ldots\nu}$ =	$1 - \mu_0$	$0 < \mathbf{a}_4^{def} < \lambda^{-1}+\lambda^{-2}$	⇒ $t(\mathbf{a}_{0\ldots\nu4})$ =	F	↑
	$\mathbf{b}_{0\ldots\nu4} = 1 - \mathbf{a}_{0\ldots\nu}$ =	$1 - \mu_0$	$0 < \mathbf{b}_4^{def} < \lambda^{-1}$	⇒ $t(\mathbf{b}_{0\ldots\nu4})$ =	F	↑
	$\mathbf{c}_{0\ldots\nu4} = -\lambda^{-1} + \mathbf{b}_{0\ldots\nu}$ =	$-\lambda^{-1} + \mu_0$	$0 < \mathbf{c}_4^{def} < \lambda^{-1}$	⇒ $t(\mathbf{c}_{0\ldots\nu4})$ =	F	↑
	$\mathbf{d}_{0\ldots\nu4} = \lambda^{-1} - \mathbf{c}_{0\ldots\nu}$ =	$\lambda^{-1} - \mu_0$	$0 < \mathbf{d}_4^{def} < \lambda^{-1}$	⇒ $t(\mathbf{d}_{0\ldots\nu4})$ =	T	↑

7. Application and outlook

Figure 6 shows a path of 33 h_k-transformations, calculated by succession algorithm. The end-cell correlates with the start-cell Ω_0 in the center of the substitution tiling, here limited by $\Omega_0 \cdot \lambda^2$.
The path is denoted by the index of the end-cell $Q_{0\bar{4}33\bar{2}\bar{4}\bar{3}\bar{2}\bar{4}\bar{3}\bar{3}\bar{3}1233\bar{2}1334234\bar{3}\bar{2}1331\bar{4}331}$. The successively calculated cells of the path correlate exactly with the globally generated substitution tiling.
The succession algorithm enables new methods of modelling quasicrystal growth. For instance it should be possible to create filigree shapes by marginal restrictions of the permitted values.
An interpretation with respect to real quasicrystal growth would be the goal, as well as the development of dodecagonal or icosahedral version types of the quasiperiodic succession algorithm, built up comparably to the presented octagonal and decagonal types.

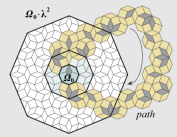

Figure 6. Successively calculated path and substitution structure

Acknowledgements: I sincerely thank Dr. Michael Willsch. His great support of the decagonal succession algorithm [7] had a sustainable effect on the present work.
I also thank Professor Christoph Richard for his very helpful corrections.

References:

[1] R. Penrose, *Math. Intell.*, **2**, (1979), 32-37
[2] N. G. de Bruijn, *Kon. Nederl. Akad. Wetensch. Proc.*, Ser. A **84**, (1981)
[3] F. P. M. Beenker, *Eindhoven Univ. Tech. TH-Report*, 82-WKS04 (1982)
[4] D. Shechtman et al., *Phys. Rev. Lett.*, **53**, (1984), 1951-1953
[5] P. Gummelt, *Geometriae Dedicata*, **62**, (1996), 1-17
[6] S. I. Ben Abraham, F. Gähler, *Phys. Rev.*, B **60**, (1999), 860-864.
[7] U. Gaenshirt, M. Willsch, *Philos. Mag.*, **87**, (2007), 3055-3065.